JACS
JOURNAL OF THE AMERICAN CHEMICAL SOCIETY
Communication
pubs.acs.org/JACS

Iterative Exponential Growth Synthesis and Assembly of Uniform Diblock Copolymers

Yivan Jiang, Matthew R. Golder, Hung V.-T. Nguyen, Yufeng Wang, Mingjiang Zhong, Jonathan C. Barnes, Deborah J. C. Ehrlich, and Jeremiah A. Johnson*

Department of Chemistry, Massachusetts Institute of Technology, 77 Massachusetts Avenue, Cambridge, Massachusetts 02139, United States

Supporting Information

ABSTRACT: Studies on the phase segregation of unimolecular block copolymers (BCPs) are limited by a lack of reliable, versatile methods for the synthesis of such polymers on the preparative scale. Herein, we describe an advancement of Iterative Exponential Growth (IEG) wherein chiral allyl-based IEG oligomers are subjected to thiol−ene reactions and converted into unimolecular BCPs. With this strategy we have synthesized uniform BCPs with molar masses up to 12.1 kDa on ∼1 g scale. BCPs composed of decane-based side chains and either triethyleneglycol- or thioglycerol-based side chains phase-segregate into hexagonal cylinder morphologies. The assembly is not driven by side-chain crystallization, but is instead the result of amorphous BCP assembly.

New synthetic approaches that facilitate access to precisely defined and diversely functionalized uniform macromolecules in useful quantities will enable the elucidation of structure−property relationships that will guide the design of next-generation polymeric materials.[1] Living statistical polymerization methods can yield polymers with precise nanoscale structures on kilogram scales, but these methods lack absolute mass control, sequence control, and stereocontrol.[2] Increased control has been achieved by using monomers with preloaded functionality,[3] by taking advantage of inherent differences in the rates of propagation between monomers,[4] by templating monomer addition,[5] or by chromatographic purification.[6] On the opposite end of the spectrum, solid-phase syntheses provide an extremely valuable tool for the synthesis of macromolecules with absolute structural control.[7] However, these methods require large excesses of reagents in each step and are not yet amenable for the synthesis of polymers in a readily scalable way.

Iterative Exponential Growth (IEG) is an alternative synthetic strategy wherein doubly protected molecules of length l undergo cycles of orthogonal activations and couplings to yield macromolecules with length $l{\cdot}2^{\#cycles}$.[8] Though IEG is limited to repetitive or palindromic sequences, it can provide unimolecular, fully sequence-controlled and stereocontrolled polymers in fewer reactions than solid-phase synthesis, and without the need for large excesses of reagents.[9]

Recently, our group reported[10] an Iterative Exponential Growth Plus Side-chain Functionalization (IEG+) strategy that allowed for the synthesis of chiral, uniform oligomers and polymers with variable sequences of acetyl (Ac) and benzyl (Bn) protected alcohols (Figure 1A). The key to IEG+ was the selection of extremely efficient reactions—nucleophilic opening of epoxides with azide, fluoride-mediated desilylation of alkynes, and copper-catalyzed azide−alkyne cycloaddition (CuAAC)—that provided macromolecules in excellent yields and with high atom economy. Nonetheless, our previous IEG+ system included only simple side-chain protecting groups; the design of macromolecules with more advanced function requires a next-generation IEG+ strategy.

Herein we report a new IEG+ strategy—allyl-IEG—that yields uniform, sequence-defined macromolecules with side-chain alkene functionalities capable of efficient post-polymerization functionalization reactions. We make use of efficient thiol−ene addition reactions to synthesize uniform BCPs (32mers) with molar masses from 9 to 12.1 kDa on ∼1 g scale. These BCPs undergo bulk microphase separation to form hexagonally packed cylinders with domain sizes that directly correlate with their molecular structures. This approach offers a simple platform for studying how molecular-level details impact a broad range of polymer properties.

Figure 2A depicts the allyl-IEG process. First, (*R*)-glycidyl propargyl ether ((***R*)-GPE**) was converted to azide **1-N$_3$** via triisopropylsilyl (TIPS) protection of the alkyne (i), nucleophilic opening of the epoxide with NaN_3 (ii), and allylation of the newly formed alcohol with allyl bromide (iii). Separately, **1-alkyne** was prepared from **(*R*)-GPE** by regioselective epoxide opening with *tert*-butyl alcohol in the presence of $Mg(ClO_4)_2$ (iv), followed by allylation with allyl bromide (v), acidic cleavage of the *tert*-butyl ether with 85% phosphoric acid (vi), tosylation of the resulting alcohol (vii), and nucleophilic substitution with LiBr (viii). Finally, **1-N$_3$** and **1-alkyne** were coupled via CuAAC in the presence of 5 mol% CuBr and 10 mol% *N*,*N*,*N*′,*N*″,*N*″-pentamethyldiethylenetriamine (PMDETA) in DMF for 2 h to yield dimer **2** in 89% isolated yield (37.9 g).

Compound **2** is a useful starting point for subsequent IEG cycles (Figure 2B). Exposure of **2** to tetrabutylammonium fluoride in THF for 15 min provided **2-alkyne**, while separate exposure of **2** to NaN_3 at 35 °C for 12 h provided **2-N$_3$**.[11] Coupling of **2-alkyne** and **2-azide** under the aforementioned CuAAC conditions gave 19.3 g of tetramer **4** (88% from **2**). Repeating this sequence with **4** as the starting material yielded octamer **8** (9.27 g, 69% from **4**) and hexadecamer **16** (3.15 g, 51% from **8**). Note that the reported yields were obtained after

Received: May 13, 2016
Published: July 12, 2016

DOI: 10.1021/jacs.6b04964
J. Am. Chem. Soc. 2016, 138, 9369−9372

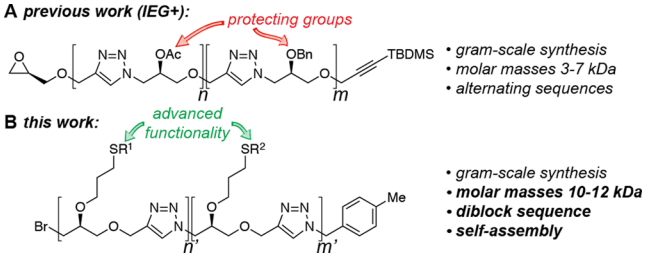

Figure 1. (A) The previous IEG+ system, though efficient and high yielding, was limited to simple protecting group functionality. (B) By utilizing thiol−ene addition reactions, we can now incorporate a larger library of functional groups into IEG+.

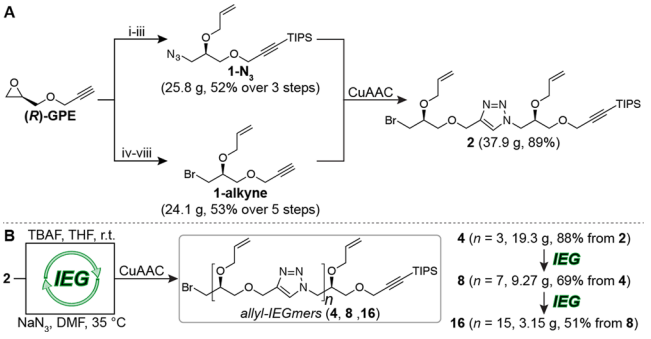

Figure 2. (A) Synthesis of allyl-IEG dimer **2** from (***R***)**-GPE**. Reagents and conditions: (i) *n*-BuLi, TIPSCl, THF, −78 °C to rt; (ii) NaN_3, AcOH, DMF, 65 °C; (iii) allyl bromide, NaH, DMF, rt; (iv) *t*-BuOH, $Mg(ClO_4)_2$, rt; (v) allyl bromide, NaH, DMF, rt; (vi) H_3PO_4, rt; (vii) TsCl, 4-DMAP, TEA, DCM, rt; (viii) LiBr, DMF, 45 °C. (B) Conditions for each IEG cycle to produce allyl-IEG tetramer **4**, octamer **8**, and hexadecamer **16**.

chromatographic purification of each oligomeric species. Furthermore, the same set of procedures was used for each coupling; the reactions were not optimized to maximize the yield for each individual allyl-IEGmer. Nonetheless, allyl-IEG enabled the production of multiple grams of **16** from **2** within 3 d.

Gel permeation chromatography (GPC) traces for **4**, **8**, and **16** were monomodal (Figure 3A, Figure S18); matrix-assisted laser desorption/ionization-time-of-flight (MALDI-TOF) mass spectra (MS) for each compound displayed a major peak that corresponded to the calculated mass plus a Na^+ or H^+ (Figure 3B). ^{1}H NMR spectroscopy further validated the structures and purity (see Supporting Information (SI)).

We next turned our efforts toward leveraging these allylated oligomers for the synthesis of BCPs. Thiol−ene radical addition is a particularly useful olefin functionalization reaction that is known for its efficiency in the context of macromolecular synthesis.[12] For example, Klok and co-workers demonstrated the use of thiol−ene additions for functionalization of uniform allylated oligoesters (up to octamers) prepared via an IEG

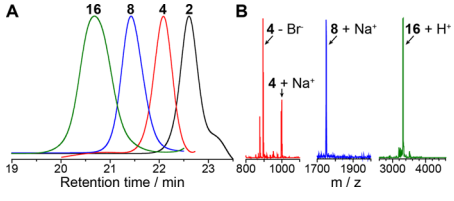

Figure 3. (A) Normalized GPC traces in DMF for allylated oligomers **2**, **4**, **8**, and **16**. (B) MALDI-MS spectra for allylated oligomers **4**, **8**, and **16**.

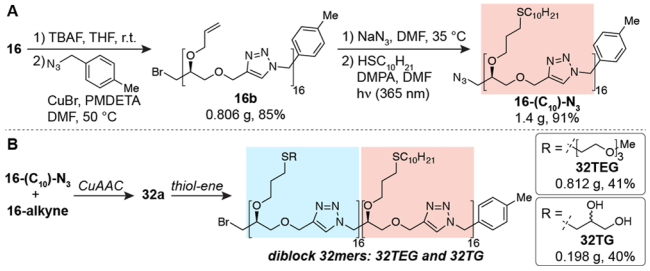

Figure 4. (A) Capping of the terminal alkyne and thiol−ene reaction of the allyl-IEG 16-mer. (B) Synthesis and thiol−ene functionalization of 32-mer BCPs.

strategy.[13] First, to avoid side reactions with the TIPS-alkyne chain end, **16** was exposed to TBAF to generate **16-alkyne**. Coupling with 4-methylbenzylazide yielded **16b**, which was converted to azide **16b-N_3** via treatment with NaN_3. A N_2-sparged DMF solution of **16b-N_3**, decanethiol (8 equiv to alkene), and 2,2-dimethoxy-2-phenylacetophenone (DMPA, 0.25 equiv) was exposed to 365 nm light for 2 h. Dialysis in ethanol (1k MWCO tubing) provided hexadecamer **16-(C_{10})-N_3** (Figure 4A). Separately, **16** was treated with TBAF to produce **16-alkyne**; the latter was coupled to **16-(C_{10})-N_3** via CuAAC to provide 1.02 g of a 32-mer BCP (**32a**) that features 16 decane side chains and 16 allyl groups. GPC (Figure 5A), MALDI-MS (Figure 5B), and ^{1}H NMR (SI) confirmed the structure of BCP **32a**.

Irradiation of **32a** in the presence of DMPA and either 1-mercapto-triethyleneglycol monomethyl ether (TEG-SH) or thioglycerol (TG-SH) provided BCPs **32TEG** and **32TG**, respectively (see SI and Figure 4B). Figure 5 shows GPC and MALDI-MS data for **32TEG** and **32TG**. The GPC trace for **32TEG** features a single peak. The GPC trace of **32TG** was broad and showed shoulder peaks due to aggregation during GPC analysis. Global acetylation of **32TG** precluded this aggregation; GPC analysis of acetylated **32TG** confirmed that it is uniform (SI, Figure S21). The MALDI spectra for **32TEG** and **32TG** show single peaks that match the calculated masses for both BCPs. Notably, **32TEG** has a mass of 12 106 Da, which we believe sets a new benchmark for non-amide or phosphate-based uniform synthetic polymers; this mass is nearly 6 kDa greater than what was achieved in our previous IEG+ work.[10]

We next sought to investigate the propensity of BCPs **32TEG** and **32TG** to undergo bulk self-assembly. BCP self-assembly is a rich field that has produced numerous fundamental discoveries and commercial applications.[14] Recent studies have elucidated the phase diagrams of unimolecular BCPs;[15] to our knowledge, no examples of bulk self-assembly of IEG-derived polymers are known. We were particularly inspired by reports from Zuckermann and co-workers, which have shown that uniform

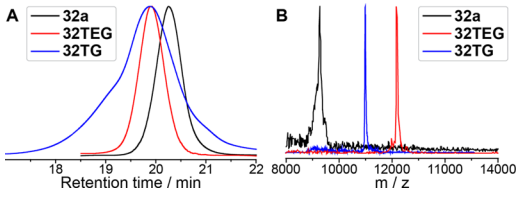

Figure 5. (A) Normalized GPC traces for diblock 32-mers **32a**, **32TEG**, and **32TG**. Note: peak broadening observed for **32TG** is due to aggregation of the glycerol blocks (see Figure S20 and S21). (B) MALDI-MS data for BCPs **32a**, **32TEG**, and **32TG**.

DOI: 10.1021/jacs.6b04964
J. Am. Chem. Soc. 2016, 138, 9369−9372

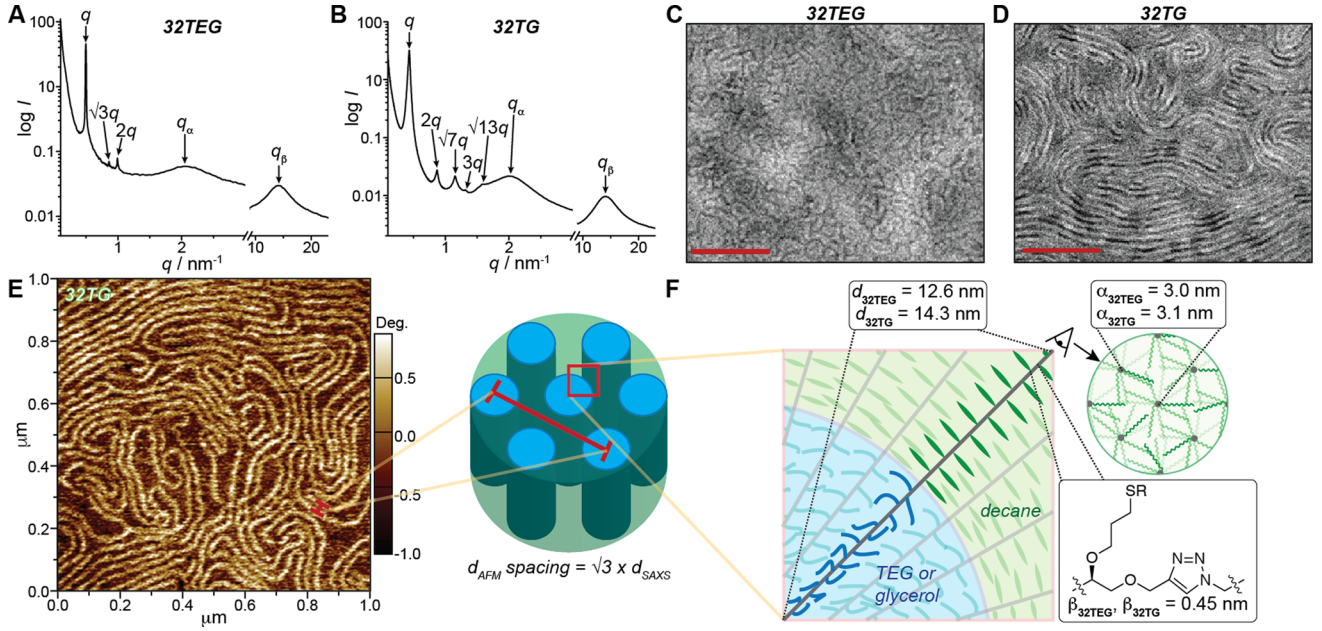

Figure 6. SAXS data with intensity versus scattering vector q for (A) **32TEG** and (B) **32TG**. TEM images (scale bar = 200 nm) of thermally annealed (C) **32TEG** and (D) **32TG**. (E) Tapping-mode AFM phase image of **32TG**. The AFM-measured d spacing corresponds to $\sqrt{3}d_{SAXS}$. (F) Cartoon illustrating a cross section of a part of a **32TEG** or **32TG** cylinder that has three distinct dimensions: the d spacing, the distance between polymer backbones α, and the length of the monomer residues β.

diblock copolypeptoids with TEG and decane blocks in their side chains form bulk lamellae.[15b] In Zuckermann's system, the authors proposed that self-assembly was driven by crystallization of the decane side chains, which enforced crystallization of the otherwise amorphous TEG side chains, and led to lamellar phases in all cases where ordering was observed. Thus, the peptoids displayed crystallinity-driven assembly, rather than traditional amorphous BCP self-assembly,[15a,16] the latter of which is driven by the immiscibility of the two blocks scaled by the product of the chain length N and the Flory–Huggins interaction parameter χ.[17] The small inter-side-chain distance (three bonds) in peptoids likely facilitates side-chain crystallization; we wondered how the IEG backbone might behave.

Differential scanning calorimetry (DSC) for **32TEG** and **32TG** showed no observable melting transitions in the range of −55 to 175 °C (SI, Figure S22), which indicated that these BCPs are amorphous and that the larger inter-side-chain distances in our IEG BCPs inhibit side-chain crystallization.

Small-angle X-ray scattering (SAXS) was used to characterize thermally annealed (see SI) samples of **32TEG** and **32TG**. The SAXS curve for **32TEG** (Figure 6A) displays a sharp and intense principal peak at q^* = 0.04975 nm^{-1} and two additional reflections at $\sqrt{3}q^*$ and $2q^*$, which is indicative of a well-ordered hexagonal cylinder (HC) morphology with a domain spacing ($d^* = 2\pi/q^*$) of 12.6 nm. The SAXS curve for **32TG** (Figure 6B) also suggests an HC morphology with a principal peak at 0.04375 nm^{-1}, which translates to a domain spacing of 14.3 nm, and reflections at $2q^*$, $\sqrt{7}q^*$, $3q^*$, and $\sqrt{13}q^*$.

Transmission electron microscopy (TEM) images of spin-coated, thermally annealed thin films of **32TEG** and **32TG** support the HC morphologies observed by SAXS. The image for **32TEG** suggests a lack of long-range order in the film (Figure 6C). The d spacing measured by TEM was 17.9 ± 0.7 nm, which is larger than the 12.6 nm measured by SAXS; this difference may be due to a difference in the film versus bulk morphology.[18] TEM analysis of **32TG** showed phase separation and long-range order (Figure 6D); a d spacing of 16.2 ± 0.5 nm was obtained, which agrees well with the SAXS value (14.3 nm).

Atomic force microscopy (AFM) was used to characterize the surface morphology of films of **32TEG** and **32TG**. In the case of **32TEG**, no contrast between the TEG and decane domains was observed. However, AFM analysis of **32TG** (Figure 6E) showed clear phase separation, indicative of the HC morphology. The AFM-measured periodicity was approximately 25.0 nm, which is notably larger than the d spacing measured by SAXS and TEM. This value agrees well with the height of the HC unit cell measured by SAXS: $\sqrt{3}d_{SAXS}$ = 24.8 nm (Figure 6E, right). These data suggest that the cylinders are composed of the higher surface energy glycerol block, while the lower surface energy decane blocks comprise the matrix.

As shown in Figure 6A,B, two broad peaks, q_α and q_β, were observed in the wide-angle X-ray scattering (WAXS) curves for both **32TEG** and **32TG**. To assign these peaks, we estimated the distances in these BCPs using Chimera (see SI): the calculated length of the decane side chains was 1.76 nm, and therefore the distance between polymer backbones would be ∼3.52 nm. This value closely matches the experimental α values, which were 3.0 nm for **32TEG** and 3.1 nm for **32TG**. The difference between calculated and experimental values could be due to intercalation of the side chains. Again using Chimera, we calculated that a fully extended monomer unit of our polymers would have a length of 0.95 nm, which is more than double the length of 0.45 nm represented by β. Assuming that β corresponds to the average monomer-to-monomer spacing, this finding suggests that the backbone is not fully extended. The backbone conformation could potentially be influenced by the chirality of the monomer units and is a subject for future study.

The estimated full end-to-end length (R) is 14.4 nm for both **32TEG** and **32TG**. These values are very close to the d-spacing of each polymer, where the ratios d/R are 0.875 and 0.993 for **32TEG** and **32TG**, respectively. These results suggest that the polymer backbones mostly maintain a straight orientation and

DOI: 10.1021/jacs.6b04964
J. Am. Chem. Soc. 2016, 138, 9369–9372

that the observed HC assembly is driven by the difference in volume fraction between the less dense decane block and the denser TEG and TG blocks (Figure 6F).

In conclusion, we have introduced a new allyl-IEG system that can serve as a basis for the bulk synthesis of unimolecular, chiral BCPs. So far these polymers have shown traditional self-assembly despite their short length, which is likely due to their unique, flexible, poly(ether-*co*-triazole) backbone. With this system in place, we seek to further explore the morphologies of these polymers beyond HCs with varying block sizes, diverse side chains, and alternating stereoconfigurations.

■ ASSOCIATED CONTENT

Supporting Information

The Supporting Information is available free of charge on the ACS Publications website at DOI: 10.1021/jacs.6b04964.

Methods, materials, and characterization data (PDF)

■ AUTHOR INFORMATION

Corresponding Author

*jaj2109@mit.edu

Notes

The authors declare no competing financial interest.

■ ACKNOWLEDGMENTS

We thank DuPont for support of this work. J.C.B. acknowledges the Howard Hughes Medical Institute (Postdoctoral Fellow of the Life Sciences Research Foundation). H.V.-T.N. thanks the National Science Foundation for a Graduate Research Fellowship. We thank the Advanced Photon source, a U.S. Department of Energy (DOE) Office of Science User Facility operated for the DOE Office of Science by Argonne National Laboratory under Contract No. DE-AC0206CH11357.

■ REFERENCES

(1) (a) Müllen, K. *Nat. Rev. Mater.* **2016**, *1*, 15013. (b) Lutz, J.-F.; Lehn, J.-M.; Meijer, E. W.; Matyjaszewski, K. *Nat. Rev. Mater.* **2016**, *1*, 16024. (c) Robertson, E. J.; Battigelli, A.; Proulx, C.; Mannige, R. V.; Haxton, T. K.; Yun, L.; Whitelam, S.; Zuckermann, R. N. *Acc. Chem. Res.* **2016**, *49*, 379. (d) Sun, H.-J.; Zhang, S.; Percec, V. *Chem. Soc. Rev.* **2015**, *44*, 3900. (e) Percec, V.; Glodde, M.; Bera, T. K.; Miura, Y.; Shiyanovskaya, I.; Singer, K. D.; Balagurusamy, V. S. K.; Heiney, P. A.; Schnell, I.; Rapp, A.; Spiess, H.-W.; Hudson, S. D.; Duan, H. *Nature* **2002**, *417*, 384. (f) Rosen, B. M.; Wilson, C. J.; Wilson, D. A.; Peterca, M.; Imam, M. R.; Percec, V. *Chem. Rev.* **2009**, *109*, 6275. (g) Rosen, B. M.; Percec, V. *Chem. Rev.* **2009**, *109*, 5069.

(2) (a) Braunecker, W. A.; Matyjaszewski, K. *Prog. Polym. Sci.* **2007**, *32*, 93. (b) Bielawski, C. W.; Grubbs, R. H. *Prog. Polym. Sci.* **2007**, *32*, 1.

(3) (a) Lienkamp, K.; Madkour, A. E.; Musante, A.; Nelson, C. F.; Nüsslein, K.; Tew, G. N. *J. Am. Chem. Soc.* **2008**, *130*, 9836. (b) Johnson, J. A.; Lu, Y. Y.; Burts, A. O.; Xia, Y.; Durrell, A. C.; Tirrell, D. A.; Grubbs, R. H. *Macromolecules* **2010**, *43*, 10326. (c) Burts, A. O.; Li, Y.; Zhukhovitskiy, A. Z.; Patel, P. R.; Grubbs, R. H.; Ottaviani, M. F.; Turro, N. J.; Johnson, J. A. *Macromolecules* **2012**, *45*, 8310. (d) Zhang, J.; Matta, M. E.; Hillmyer, M. A. *ACS Macro Lett.* **2012**, *1*, 1383. (e) Gutekunst, W. R.; Hawker, C. J. *J. Am. Chem. Soc.* **2015**, *137*, 8038.

(4) (a) Schmidt, B. V. K. J.; Fechler, N.; Falkenhagen, J.; Lutz, J.-F. *Nat. Chem.* **2011**, *3*, 236. (b) Zamfir, M.; Lutz, J.-F. *Nat. Commun.* **2012**, *3*, 1138. (c) Kramer, J. W.; Treitler, D. S.; Dunn, E. W.; Castro, P. M.; Roisnel, T.; Thomas, C. M.; Coates, G. W. *J. Am. Chem. Soc.* **2009**, *131*, 16042.

(5) (a) Hibi, Y.; Ouchi, M.; Sawamoto, M. *Angew. Chem., Int. Ed.* **2011**, *50*, 7434. (b) Ida, S.; Ouchi, M.; Sawamoto, M. *Macromol. Rapid Commun.* **2011**, *32*, 209.

(6) (a) Schmitz, F. P.; Klesper, E. *J. Supercrit. Fluids* **1990**, *3*, 29. (b) Macko, T.; Pasch, H.; Wang, Y. *Macromol. Symp.* **2009**, *282*, 93. (c) Lawrence, J.; Lee, S.-H.; Abdilla, A.; Nothling, M. D.; Ren, J. M.; Knight, A. S.; Fleischmann, C.; Li, Y.; Abrams, A. S.; Schmidt, B. V. K. J.; Hawker, M. C.; Connal, L. A.; McGrath, A. J.; Clark, P. G.; Gutekunst, W. R.; Hawker, C. J. *J. Am. Chem. Soc.* **2016**, *138*, 6306.

(7) (a) Merrifield, R. B. *J. Am. Chem. Soc.* **1963**, *85*, 2149. (b) Wojcik, F.; Ponader, D.; Mosca, S.; Hartmann, L. *ACS Symp. Ser.* **2014**, *1170*, 85. (c) Al Ouahabi, A.; Charles, L.; Lutz, J. F. *J. Am. Chem. Soc.* **2015**, *137*, 5629.

(8) Binauld, S.; Damiron, D.; Connal, L. A.; Hawker, C. J.; Drockenmuller, E. *Macromol. Rapid Commun.* **2011**, *32*, 147.

(9) (a) Paynter, O. I.; Simmonds, D. J.; Whiting, M. C. *J. Chem. Soc., Chem. Commun.* **1982**, *20*, 1165. (b) Zhang, J. S.; Moore, J. S.; Xu, Z. F.; Aguirre, R. A. *J. Am. Chem. Soc.* **1992**, *114*, 2273. (c) Schumm, J. S.; Pearson, D. L.; Tour, J. M. *Angew. Chem., Int. Ed. Engl.* **1994**, *33*, 1360. (d) Lengweiler, U. D.; Fritz, M. G.; Seebach, D. *Helv. Chim. Acta* **1996**, *79*, 670. (e) Li, G. R.; Wang, X. H.; Wang, F. S. *Tetrahedron Lett.* **2005**, *46*, 8971. (f) Takizawa, K.; Tang, C.; Hawker, C. J. *J. Am. Chem. Soc.* **2008**, *130*, 1718. (g) Huang, B.; Hermes, M. E. *J. Polym. Sci., Part A: Polym. Chem.* **1995**, *33*, 1419. (h) Cai, C. Z.; Vasella, A. *Helv. Chim. Acta* **1996**, *79*, 255. (i) Liess, P.; Hensel, V.; Schluter, A. D. *Liebigs Ann.* **1996**, *1996*, 1037. (j) Percec, V.; Asandei, A. D. *Macromolecules* **1997**, *30*, 7701. (k) Sadighi, J. P.; Singer, R. A.; Buchwald, S. L. *J. Am. Chem. Soc.* **1998**, *120*, 4960. (l) Louie, J.; Hartwig, J. F. *Macromolecules* **1998**, *31*, 6737. (m) Williams, J. B.; Chapman, T. M.; Hercules, D. M. *Macromolecules* **2003**, *36*, 3898. (n) Zhou, C. Z.; Liu, T. X.; Xu, J. M.; Chen, Z. K. *Macromolecules* **2003**, *36*, 1457. (o) Binauld, S.; Hawker, C. J.; Fleury, E.; Drockenmuller, E. *Angew. Chem., Int. Ed.* **2009**, *48*, 6654. (p) Leibfarth, F. A.; Johnson, J. A.; Jamison, T. F. *Proc. Natl. Acad. Sci. U. S. A.* **2015**, *112*, 10617. (q) Li, X.; Qi, T.; Srinivas, K.; Massip, S.; Maurizot, V.; Huc, I. *Org. Lett.* **2016**, *18*, 1044.

(10) Barnes, J. C.; Ehrlich, D. J. C.; Gao, A. X.; Leibfarth, F. A.; Jiang, Y.; Zhou, E.; Jamison, T. F.; Johnson, J. A. *Nat. Chem.* **2015**, *7*, 810.

(11) We noticed temperatures past 35 °C led to gradual cyclization of the terminal azide with the neighboring alkene, preventing reaction in the CuAAC coupling reaction. Selected examples of this intramolecular cyclization: (a) Bennett, R. B., III; Choi, J. R.; Montgomery, W. D.; Cha, J. K. *J. Am. Chem. Soc.* **1989**, *111*, 2580. (b) Zhou, Y.; Murphy, P. V. *Org. Lett.* **2008**, *10*, 3777. (c) Hui, B. W.-Q.; Chiba, S. *Org. Lett.* **2009**, *11*, 729.

(12) (a) Campos, L. M.; Killops, K. L.; Sakai, R.; Paulusse, J. M. J.; Damiron, D.; Drockenmuller, E.; Messmore, B. W.; Hawker, C. J. *Macromolecules* **2008**, *41*, 7063. (b) Hoyle, C. E.; Bowman, C. N. *Angew. Chem., Int. Ed.* **2010**, *49*, 1540.

(13) Franz, N.; Menin, L.; Klok, H.-A. *Eur. J. Org. Chem.* **2009**, 5390.

(14) (a) Bates, F. S.; Hillmyer, M. A.; Lodge, T. P.; Bates, C. M.; Delaney, K. T.; Fredrickson, G. H. *Science* **2012**, *336*, 434. (b) Muthukumar, M.; Ober, C. K.; Thomas, E. L. *Science* **1997**, *277*, 1225. (c) Lynd, N. A.; Hillmyer, M. A. *Macromolecules* **2005**, *38*, 8803. (d) Bates, C. M.; Seshimo, T.; Maher, M. J.; Durand, W. J.; Cushen, J. D.; Dean, L. M.; Blachut, G.; Ellison, C. J.; Willson, C. G. *Science* **2012**, *338*, 775. (e) Thomas, T. S.; Hwang, W.; Sita, L. R. *Angew. Chem., Int. Ed.* **2016**, *55*, 4683.

(15) (a) van Genabeek, B.; de Waal, B. F. M.; Gosens, M. M. J.; Pitet, L. M.; Palmans, A. R.; Meijer, E. W. *J. Am. Chem. Soc.* **2016**, *138*, 4210. (b) Sun, J.; Teran, A. A.; Liao, X.; Balsara, N. P.; Zuckermann, R. N. *J. Am. Chem. Soc.* **2014**, *136*, 2070. (c) Sun, J.; Jiang, X.; Lund, R.; Downing, K. H.; Balsara, N. P.; Zuckermann, R. N. *Proc. Natl. Acad. Sci. U. S. A.* **2016**, *113*, 3954. (d) Zha, R. H.; de Waal, B. F. M.; Lutz, M.; Teunissen, A. J. P.; Meijer, E. W. *J. Am. Chem. Soc.* **2016**, *138*, 5693.

(16) Rangarajan, P.; Register, R. A.; Fetters, L. J. *Macromolecules* **1993**, *26*, 4640.

(17) (a) Flory, P. J. *Principles of Polymer Chemistry*; Cornell University Press: Ithaca, NY, 1953. (b) Bates, F. S.; Fredrickson, G. H. *Phys. Today* **1999**, *52*, 32.

(18) Bang, J.; Jeong, U.; Ryu, D. Y.; Russell, T. P.; Hawker, C. J. *Adv. Mater.* **2009**, *21*, 4769.

DOI: 10.1021/jacs.6b04964
J. Am. Chem. Soc. 2016, 138, 9369−9372